Development of in-house phantoms using polyester resin and methyl ethyl ketone peroxide materials: Investigation of their CT numbers for various tube voltages and field of views

Luthfi Nurrahma Shofiana[1], Choirul Anam[1*], Heri Sutanto[1], RinHafsahtul Asiah[1], Riski Nihayati[1], Ansory Khaerul[2], Geoff Dougherty[3]

[1]Department of Physics, Faculty of Sciences and Mathematics, Diponegoro University, Tembalang, Semarang, Indonesia
[2]Department of Radiology, Koja Hospital, Jakarta, Indonesia
[3]Department of Applied Physics and Medical Imaging, California State University Channel Islands, Camarillo, CA 93012, USA

*)Corresponding author: anam@fisika.fsm.undip.ac.id

ARTICLE INFO

ABSTRACT

We developed in-house phantoms of various sizes from polyester resin (PR) and methyl ethyl ketone peroxide (MEKP) and investigated the CT numbers of the phantoms for various tube voltages and reconstructed fields of view (FOV). In-house phantoms with diameters of 8, 16, 24, and 32 cm were developed. The phantoms were made using99.7% PR and 0.3% MEKP by weight. The phantoms were scanned with a Siemens SOMATOM Emotion 6 CT scanner for various tube voltages (i.e., 80, 110 and 130 kVp) and fields of view (FOVs) (i.e., 35, 40, 45, and 50 cm). CT numbers were found to be in the range 86to 147 HU. The CT numbers of the phantoms depend on diameter and tube voltage but are independent of FOV.

1. Introduction

Computed tomography (CT) is a valuable diagnostic tool that is widely used in healthcare system [1, 2]. CT can advance the making an accurate diagnosis, limiting unnecessary medical processes, and increasing an effectiveness of treatment [3]. However, CT provides radiation dose to patients, and may induce cancer in the future. Although the probability of cancer appearance is very small, its impact is not negligible [4-6]. Concern about the increasing use of CT and the resulting impact on radiation dose from it continues to fuel high interest.

The radiation dose of CT is usually estimated by standardized phantom, made from the polymethyl methacrylate (PMMA) material. The standard PMMA phantom has two diameters, 32 cm (body phantom) and 16 cm (head phantom)[7, 8]. By using these two phantoms, the output of the CT in terms of volume CT dose index (CTDIvol) is easily measured [9].

It is worthnoting that CTDIvol is only valid in limited conditions, if implemented to the patient. This is because each patient is unique and there are no standardized phantoms to fit all patients. In terms of radiation dose, a size-specific dose estimate (SSDE) has been proposed for estimating the radiation dose for an individual patient undergoing a CT examination [10]. The SSDE is designed to be as simple as possible to make it easily implemented in the daily clinical setting [11-12].

The accuracy of SSDE has been investigated by many researchers [13, 14]. Investigation of the accuracy of SDDE requires the availability of phantoms of different sizes. Choi et al [15] developed in-house phantoms with various diameters (i.e. 12, 16, 20, and 24 cm) made from PMMA material. Adhianto et. al. [16] also developed phantoms from PMMA material with various diameters (i.e., 8, 16, 24, 32, and 40 cm).

Efforts to develop an alternative low-priced alternative to the standard PMMA phantom are necessary. Alternative materials such as nylon [17] and polyester resin (PR) [18] have been established previously. Hilmawati et. al. [18] and Asiah et. al. [19] developed a phantom for CTDIvol measurement with a diameter of 16 cm, made from inexpensive available materials, i.e., PR and methyl ethyl ketone peroxide (MEKP) as catalyst. It was reported that the best composition of MEKP in the PR is 0.3wt%, which gave results comparable to the standard PMMA phantom [18]. The CTDIvol of PR-MEKP phantom was only 5% lower than the PMMA phantom. PR is a widely used polymer and its density is similar to that of human tissue, i.e., 1.10-1.15 g.cm^{-3} [20]. The PR is non-toxic, insoluble, resistant to water absorption, transparent, and easy to manipulate without sophisticated equipment [21].

Based on previous works [16, 18, 19], we developed in-house phantoms from PR and MEKP for various diameters. We then scanned the phantoms with different tube voltages and field of views (FOV). In this study we investigated their CT numbers for each diameter, for various tube voltages and FOVs. CT number is the pixel value of the CT image which represents the linear attenuation

coefficient of the phantoms [22-24]. We will investigate the accuracy of SSDE using these phantoms in the next work.

2. Methods

2.1. Development of phantoms

In order to simulate patients with different sizes from newborns to adults, we used in-house phantoms with diameters of 8, 16, 24, and 32 cm. The phantoms were made from 99.7% PR and 0.3 % MEKP as had been proposed and investigated by previous studies [18, 19]. This composition was reported the most comparable to a PMMA phantom [18, 19].

The procedure for constructing the phantoms was similar to a previous study [18]. A schematic diagram is shown in Fig.1. Volumes of samples corresponding to 99.7% PR and 0.3 wt% MEKP for each diameter were measured and slowly stirred. They were mixed for 3 minutes using a spatula and poured into cylindrical molds (with diameters of 8, 16, 24, and 32 cm) to dry at room temperature (27°C) for about 36 hours. The dried phantoms were lathed to make small holes for pencil ion chambers in CTDIvol measurement. Each phantom had five holes, i.e. four holes at the periphery and one hole in the center. The diameter of each hole was 13.5 mm. The peripheral holes were located 10 mm from the edge of the phantoms. The outside of the phantoms was sanded to smooth them and to ensure that their diameters were 8, 16, 24 and 32 cm.
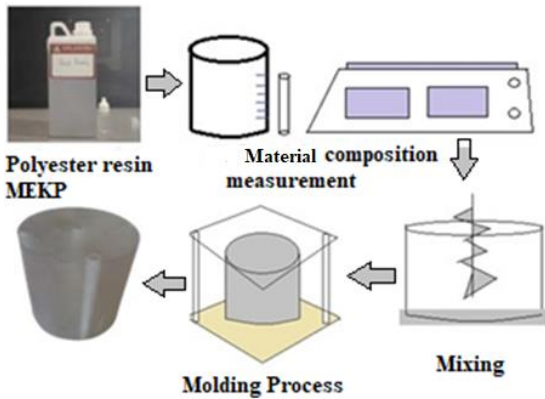
Fig .1: Schematic diagram of development of the in-house phantoms based on polyester resin (PR) and methyl ethyl ketone peroxide (MEKP).

2.2. Exposure conditions

The phantoms were scanned using a Siemens SOMATOM Emotion 6 CT scanner at Koja Hospital, North Jakarta, Indonesia (Fig. 2.). The tube voltage and FOV were varied to evaluate the effects of various exposure conditions on consistency of CT number. The tube voltages were 80, 110and 130 kVp, at a fixed FOV of 35 cm. The reconstructed FOVs were 35, 40, 45, and 50cm at a fixed tube voltage of 80 kVp. The protocol used was adult abdomen. The tube loadings were automatically adjusted to 24, 31, 67, and 237mAs for phantom sizes of 8, 16, 24, and

32 cm, respectively, using tube current modulation (TCM). We used axial mode with a slice thickness of 1.0 mm.

Fig. 2: A photograph of the 32-cm in-house phantom in a Siemens SOMATOM Emotion 6 CT scanner at Koja Hospital.

2.3. Evaluation parameters

In this study, CT numbers were measured. The average CT numbers in Hounsfield unit (HU) were measured using five square regions of interest (ROIs) each of 900 pixels (Fig. 3). The CT numbers were calculated as an average of all CT numbers within the ROI. In addition, image noise was also calculated as the standard deviation (SD) of all CT numbers within the ROI. The measurements used Philips software version 3.0.

$$CT\ number = \sum_{i=1}^{N} \frac{CT\ number_i}{N} \qquad (1)$$

$$SD = \sqrt{\frac{1}{N} \sum_{i=1}^{N} (CT\ number_i - \overline{CT\ number})^2} \qquad (2)$$

N indicated the number of pixels within the ROI.
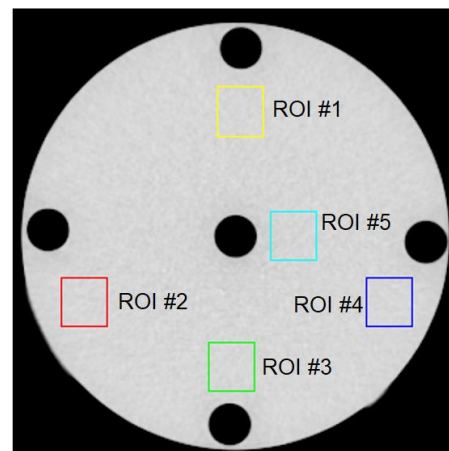
Fig. 3: Regions of interest (ROIs) for measuring CT number. The ROIs are square shapes of size 900 pixels.

3. Results and Discussions

The in-house phantoms are shown in Fig. 4. They were scanned with various tube voltages and FOVs. The images at a FOV of 35 cm and tube voltage of 80 kVp are depicted in Fig. 5. The results of the mean CT numbers for various diameters and tube voltages are tabulated in Table 1. Graphs of the mean CT number as a function of tube voltage for various diameters for every ROI are shown in Fig. 6. The mean CT numbers increase with increased tube voltage for every diameter. It is also seen that the mean CT numbers increase with increased diameter for every tube voltage.
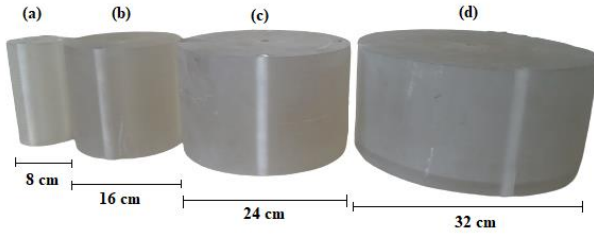
Fig. 4: In-house phantoms made from the polyester resin (PR) and methyl ethyl ketone peroxide (MEKP) with various diameters. (a) 8 cm, (b) 16 cm, (c) 24 cm, and (d) 32 cm.
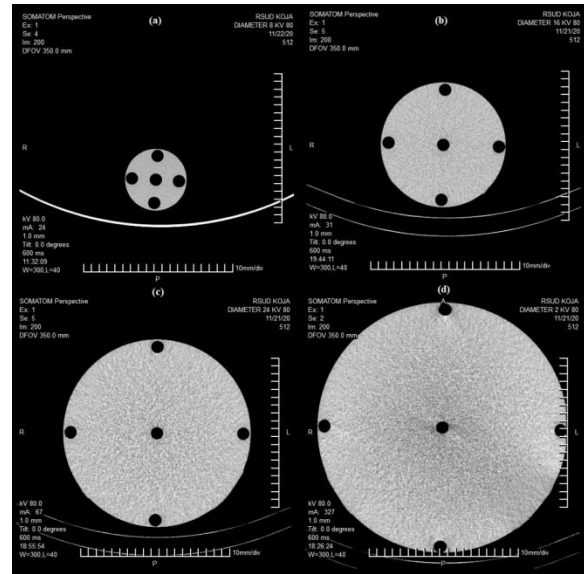
Fig. 5: Images of in-house phantoms made from polyester resin (PR) and methyl ethyl ketone peroxide (MEKP) at a field of view (FOV) of 35 cm and tube voltage of 80 kVp, for various diameters. (a) 8 cm, (b) 16 cm, (c) 24 cm and (d) 32 cm.

Table 1. Mean CT number and noise (standard deviation, SD) of the in-house phantoms for various diameters and tube voltages, at FOV of 35 cm.

| Phantom diameter (cm) | Tube voltage (kVp) | ROI #1 | | ROI #2 | | ROI #3 | | ROI #4 | | ROI #5 | | Mean HU |
		Mean (HU)	SD (HU)	Mean (HU)	SD (HU)	Mean (HU)	SD (HU)	Mean (HU)	SD (HU)	Mean (HU)	SD (HU)	
8	80	91	8.1	95	7.8	86	7.4	87	8.9	86	7.0	89.0
	110	110	5.4	121	5.2	114	5.6	118	5.7	118	5.1	116.2
	130	115	4.5	131	4.9	121	4.8	121	4.2	123	4.2	122.2
16	80	109	18.1	108	17.8	108	18.9	105	16.2	101	20.4	106.2
	110	133	10.9	130	10.5	128	12.1	125	11.6	123	14.2	127.8
	130	143	10.2	144	8.6	144	10	144	9.3	143	12.0	143.6
24	80	117	22.6	115	22.5	115	25.1	118	25.9	109	34.8	114.8
	110	136	15.5	137	14.5	134	17.2	139	15.3	130	23.7	135.2
	130	142	10.4	144	9.1	144	10.6	144	9.6	144	11.4	143.6
32	80	117	26.9	123	22.4	121	26	120	28.2	114	31.6	119.0
	110	141	18.4	141	18.7	138	21	144	17.8	138	31.6	140.4
	130	147	18.9	146	16.0	141	18.3	144	17.7	141	29.9	143.8
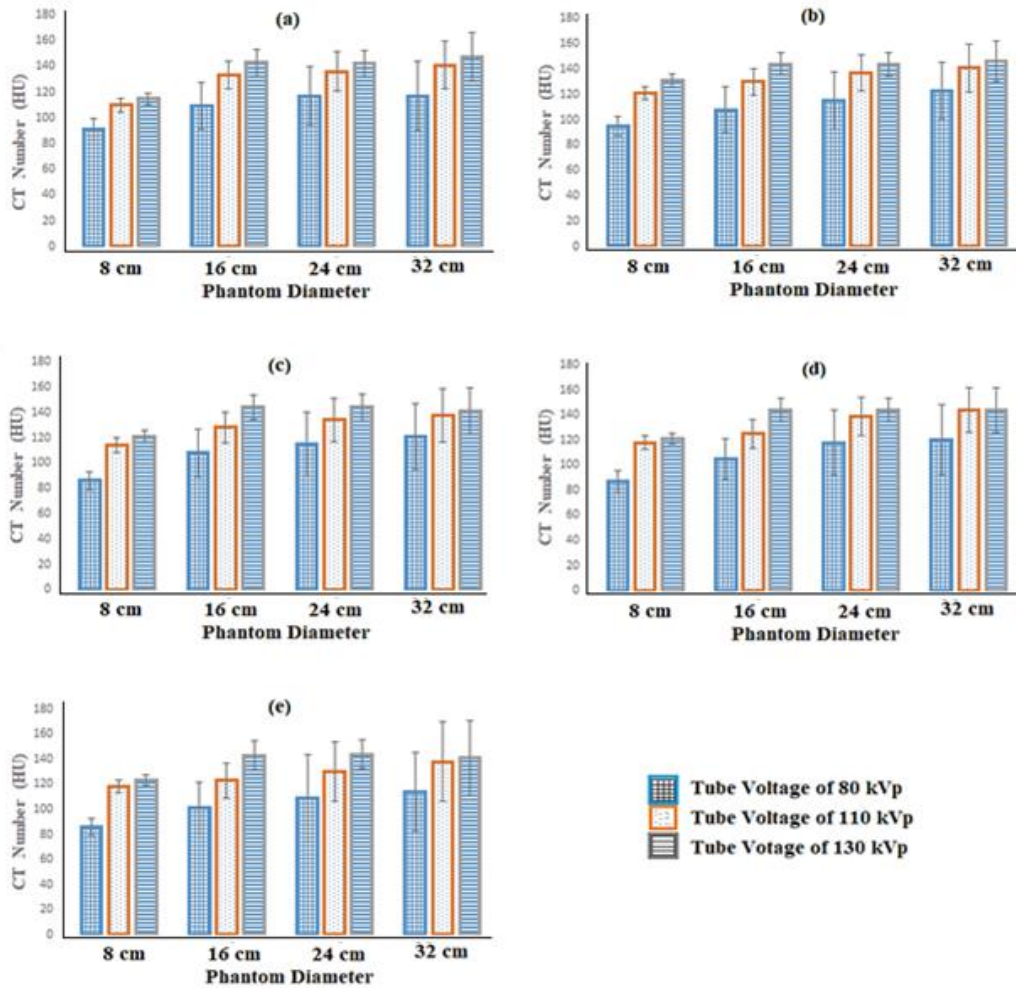
Fig. 6: Graphs of the mean CT number asa function of various tube voltage for various diameter with a fixed field of view (FOV) of 35 cm, a. Region of interest (ROI) #1, b. ROI #2, c.ROI #3, d. ROI #4, e. ROI #5.

The mean CT number for various diameters and FOVs at a fixed tube voltage of 80 kVp is tabulated in Table 2. Graphs of the mean CT number as a function of ROI for every diameter are depicted in Fig. 7. They show that the mean CT numbers are independent of FOV for every diameter.

Table 2. Mean CT number and noise (standard deviation, SD) of the in-house phantoms for various diameters and FOVs, at a fixed tube voltage of 80 kVp.

Phantom Diameter (cm)	Field of view (cm)	ROI #1		ROI #2		ROI #3		ROI #4		ROI #5		Mean HU
		Mean (HU)	SD (HU)	Mean (HU)	SD (HU)	Mean (HU)	SD (HU)	Mean (HU)	SD (HU)	Mean (HU)	SD (HU)	
8	35	91	8.1	95	7.8	86	7.4	87	8.9	86	7.0	89.0
	40	99	7.6	104	7.1	103	6.9	103	7.2	102	6.6	102.2
	45	100	7.2	103	7.8	103	6.9	102	6.6	102	6.4	102.0
	50	99	7.1	102	6.5	105	7.4	105	7.3	101	8.3	102.4
16	35	109	18.1	108	17.8	108	18.9	105	16.2	101	20.4	106.2
	40	113	17.6	115	16.9	115	19.1	117	16.2	113	21.0	114.6
	45	113	17.3	115	16.7	115	18.0	116	15.7	114	19.8	114.6
	50	114	17.2	115	17.3	115	18.5	116	16.6	114	19.3	114.8
24	35	117	22.6	115	22.5	115	25.1	118	25.9	109	34.8	114.8
	40	115	24.7	117	25.1	114	28.2	115	26.5	111	33.4	114.4
	45	116	24.3	115	25.0	115	27.8	116	27.9	111	33.6	114.6
	50	116	24.1	116	24.5	115	25.8	116	26.2	111	32.9	114.8
32	32	117	26.9	123	22.4	121	26	120	28.2	114	31.6	119.0
	40	119	25.5	115	26.9	111	26.8	117	24.6	112	33.6	114.8
	45	117	24.9	115	24.0	109	26.7	118	26.2	111	30.5	114.0
	50	118	26.3	116	23.5	111	25.4	114	25.8	111	31.4	114.0
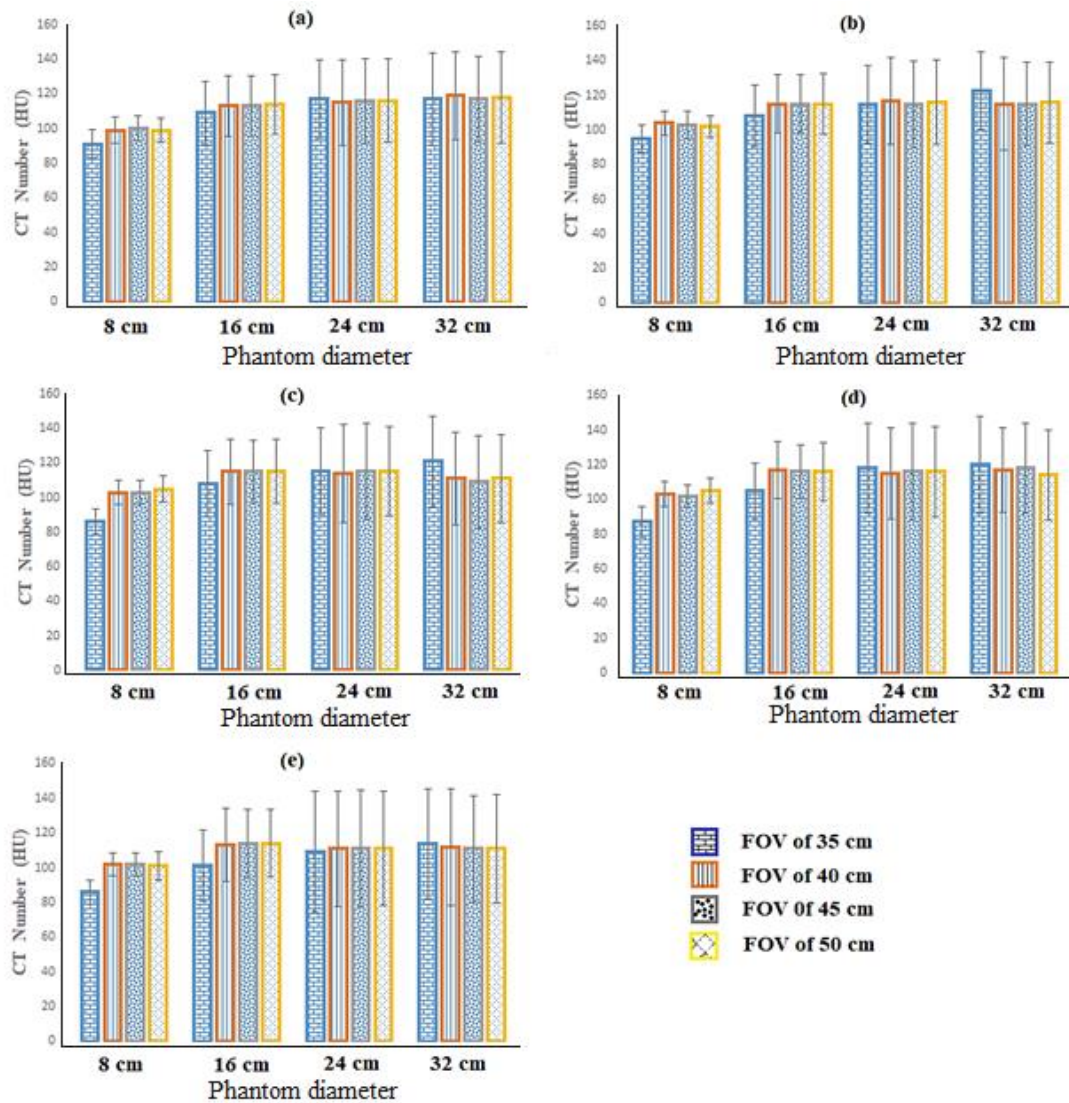
Fig. 7: Graphs of the CT number as a function of field of view (FOV) for various diameters, at a fixed tube voltage of 80 kVp, a. Region of interest (ROI) #1, b. ROI #2, c. ROI #3, d. ROI #4, and e. ROI #5.

The mean CT number of the in-house phantomsfor tube voltages 80 kVp, at FOV of 35 cm and diameter of 8 cm was 98.0 HU. For a diameter of 16 cm it was 106.2 HU, for a diameter of 24 cm it is 114.8 HU, and for a diameter of 32 cm it was 119.0 HU. It was found that the CT number increaseswith an increase of diameter and tube voltage.

We found that the CT numbers increase with the increase of diameter from 8 cm to 32 cm for all available tube voltages. This may be due to the beam hardening phenomenon [25]. At a larger diameter of the phantom, the radiation beam has a higher effective energy because lower energy is more absorbed by the phantom. At a higher effective energy rate, the linear attenuation coefficient value becomes higher, resulting in an increase in the CT number value. This is consistent with the increase in CT number at higher tube voltages due to the higher effective energy.

We also found that CT numbers increase with increasing tube voltage from 80 kVp to 130 kVp. This phenomenon was observed for all the available diameters. It depends on the material, since every

material has an effective atomic number and specific linear attenuation coefficient. Previously, Cropp et al [26] reported that CT numbers of some materials such as polyethylene and acrylic increase with an increase of tube voltage from 80 kVp to 140 kVp using 12 CT scanner models from 3 manufacturers (General Electrics (GE), Toshiba, and Siemens). On the other hand, the CT number in some materials such as bone decreases with an increase of tube voltage. Suyudi et al [27] also reported that CT numbers of nylon and acrylic increase with an increase of tube voltage from 80 kVp to 135 kVp using a Toshiba Alexian-6 CT scanner, using filtered-back projection (FBP) and iterative reconstruction (IR).

Our in-house phantoms were scanned with various reconstructed FOVs from 35, 40, 45, 50 cm at a tube voltage 80 kVp. It was found that the CT number is independent of FOV.

A previous study [18] reported that a head CTDI phantom (16 cm) made from PR and MEKP had CT numbers from 134 to 141 HU depending on ROI

position, compared with CT numbers of a PMMA phantomfrom 131 to 133 HU.

This work has some limitations. The purpose of developing this phantom was for dose measurement, butwe only investigated the CT number.The dose measurement (SSDE) using the phantoms will be conducted in asubsequentstudy. The evaluation of the phantoms was only performed on one CT scanner.

4. Conclusion

In-house phantoms based onPR andMEKP with various diameters from 8 cm to 32 cm have been successfully developed. Their CT numbers for various FOVs and tube voltages were in the range of 86 to147 HU. The CT number increased with increases in diameter and tube voltage andwas independent of FOV.

5. Conflict of Interest

The authors declare that they have no conflict of interest.

References

[1] A. T. Davis, A. L. Palmer, and A. Nisbet, "Can CT scan protocols used for radiotherapy treatment planning be adjusted to optimize image quality and patient dose? A systematic review," *Br. J. Radiol.*, **90**, 20160406, (2017).

[2] C. Anam, W. S. Budi, K. Adi, H. Sutanto, F. Haryanto, M. H. Ali, T. Fujibuchi,and G. Dougherty, "Assessment of patient dose and noise level of clinical CT images: automated measurement," *J. Radiol. Prot.*, **39,** 783-93 (2019).

[3] E. Seeram, "Computed Tomography: Physical Principle, Clinical Application, and Quality Control," *4th ed. Australia: Elsevier*, (2009).

[4] C. J. Martin, "Management of patient dose in radiology in the UK," *Rad. Prot.Dosim.*, **147,** 355-372, (2011).

[5] G. Le Coultre, J. Bize, M. Champendal, D. Wittwer, N. Ryckx, A. Aroua, P. Trueb, and R. F. Verdun, "Exposure of the Swiss population by radiodiagnostics: 2013 review," *Radiat. Prot. Dosim.*, **169**, 221-224, (2016).

[6] R. A. Parry, S. A. Glaze, and B. R. Archer, "The AAPM/RSNA Physics Tutorial for Resident.Typical patient radiation doses in diagnostic radiology" *RadioGraphics.*, **19,** 1289-1302, (1999).

[7] C. Levi, J. E. Gray, E. X. McCullough, and R. R. Hattery, "The unreliability of CT numbers as absolute values," *Am. J. Radiol.*, **139,** 443–447, (1982).

[8] C. Anam, T. Fujibuchi, F. Haryanto, R. Widita, I. Arif, and G. Dougherty, "An evaluation of computed tomography dose index measurements using a pencil ionisation chamber and small detectors," *J. Radiol. Prot.*, **39**, 112–124, (2019).

[9] S. Mubarok, L. E. Lubis, and S. A. Pawiro, "Parameter-based estimation of CT dose index and image quality using an in-house Android™-based software," *J. Phys: Conf. Ser.*, **694,** 012037, (2016).

[10] C. H. McCollough, S. Leng, L. Yu, D. D. Cody, J. M. Boone, and M. F. McNitt Gray, "CT dose index and patient dose: they are not the same thing," *Radiology*, **259,** 311-316, (2011).

[11] C. Anam, F. Haryanto, R. Widita, I. Arif and G. Dougherty, "Automated calculation of water-equivalent diameter (Dw) based on AAPM task group 220," *J. Appl. Clin. Med. Phys.*, **17,** 320-333, (2016).

[12] C. Anam, F. R. Mahdani, W. K. Dewi, H. Sutanto, P. Triadyaksa, F. Haryanto, and G. Dougherty, "An improved method for automated calculation of the water-equivalent diameter for estimating size-specific dose in CT," *J. Appl. Clin. Med. Phys.*, **22**, 313–323, (2021).

[13] C. Anam, D. Adhianto, H. Sutanto, K. Adi, M. H. Ali, W. I. D. Rae, T. Fujibuchi, and G. Dougherty, "Comparison of central, peripheral, and weighted size-specific dose in CT," *J. Xray. Sci. Technol.*, **28,** 695-708, (2020).

[14] M. Nasir, D.Pratama, C. Anam, and F. Haryanto, "Calculation of size specific dose estimates (SSDE) value at cylindrical phantom from CBCT Varian OBI v1.4 X-ray tube EGSnrc Monte Carlo simulation based," *J. Phys.: Conf. Ser.*, **694**, 012040, (2016).

[15] H. R. Choi, R. E. Kim, C. W. Heo, C. W. Kim, M. S. Yoo, and Y. Lee, "Optimization of dose and image quality using self-produced phantom with various diameters in pediatric abdominal CT scan," *Optik.*, **168,** 54-60, (2018).

[16] D. Adhianto, C. Anam, H. Sutanto, and M. H. Ali, "Effect of Phantom Size and Tube Voltage on the size-conversion factor for patient dose estimation in computed tomography examinations," *Iran. J. Med. Phys.*, **17,** 282-288, (2020).

[17] S. Sookpeng, P. Cheebsumon, T. Pengpan, and C. Martin, "Comparison of computed tomography dose index in polymethyl methacrylate and nylon dosimetry phantoms," *J. Med. Phys.*, 41, 45-51, (2016).

[18] R. Hilmawati, H. Sutanto, C. Anam, Z. Arifin, R. H. Asiah, and J. W. Soedarsono, "Development of a head CT dose index (CTDI) phantom based on polyester resin and methyl ethyl ketone peroxide (MEKP): a preliminary study," *J. Radiol. Prot.*,**40**, 544-553, (2020).

[19] R. H. Asiah, H. Sutanto, C. Anam, Z. Arifin, Bahrudin, and R. Hilmawati, "Development of In-house head computed tomography dose index phantom based on polyester-resin

materials," *Iran. J. Med. Phys.*, **18**, 255-262, (2021).

[20] W. J. Meredith and J. B. Massey, "Fundamental Physics of Radiology," *Butterworth-Heinemann*, (2013).

[21] K. Strzelec, "Studies on the properties of epoxy resins cured with polythiourethanes," *I. J. Adhesion and Adhesives.*, 27, 92-101, (2007).

[22] E. A. Zerhouni, J. F. Spivey, R. H. Morgan, F. P. Leo, F. P. Stitik, and S. S. Siegelman, "Factors influencing quantitative CT measurements of solitary pulmonary nodules," *J.Comput. Assist. Tomogr.*, 6, 1075–1087, (1982).

[23] T. B. Hunter, G. D. Pond, and O. Medina, "Dependence of substance CT number on scanning technique and position within scanner," *Comput. Radiol.* **7**, 199–203, (1983).

[24] J. T. Bushberg, J. A. Seibert, E. M. Leidholdt, and J. M. Boone, "The essential physics of medical imaging," *3rd ed. Philadelphia, PA: Lippincott Williams & Wilkins*, (2012).

[25] T.He, X. Qian, R. Zhai, and Z. Yang, "Computed tomography number measurement consistency under different beam hardening conditions: Comparison between dual-energy spectral computed tomography and conventional computed tomography imaging in phantom experiment," *J. Comput. Assist. Tomogr.*, 39, 981–985, (2015).

[26] R. J. Cropp, P. Seslija, D. Tso, and Y. Thakur, "Scanner and kVp dependence of measured CT numbers in the ACR CT phantom," *J. Appl. Clin. Med. Phys.*, 14, 338-349, (2013).

[27] I. Suyudi, C. Anam, H. Sutanto, P. Triadyaksa, and T. Fujibuchi, "Comparisons of Hounsfield unit linearity between images reconstructed using an adaptive iterative dose reduction (AIDR) and a filter back-projection (FBP) techniques," *J. Biomed. Phys. Eng.*, **10**, 215-224, (2020).